

SPACE VECTOR PWM CONTROL OF DUAL INVERTER FED OPEN-END WINDING INDUCTION MOTOR DRIVE

E.G.Shivakumar, K.Gopakumar, S.K.Sinha, Andrei Pittet, V.T.Ranganathan
[CEDT, Indian Institute of Science, Bangalore – 560 012, INDIA]

Abstract:

A space vector PWM technique is developed based on the combination of space vectors from dual inverters feeding the induction motor from both ends (open-end winding without neutral point). A total of 64 voltage space vector combinations are available for PWM voltage control of the inverter fed machine with open-end winding. A space phasor based PWM scheme is proposed with minimum number of switching in a cycle per inverter coupled with equal number of switching for each inverter.

1. INTRODUCTION

In multi level configurations (3-level as well as 5-level configurations) as the level increases, the power circuit complexity and cost increases [1,2,5]. Multilevel converters with series-connected H-bridges are suggested for high-resolution voltage phasor generation [6]. In this paper a combination of two 2-level inverters (with half the DC link voltage when compared to a conventional single inverter scheme) with open-end winding for three phase induction motor is proposed.

A combination of two 2-level inverters with three phase open-end winding induction motor results in 64 switching state vectors. This higher number of switching state vectors can be appropriately utilized generating a PWM waveform with reduced inverter switching frequency. In the present implementation isolated transformers [3] have been used for both inverters. The

scheme proposed here makes the individual inverter switching frequency equal to half of the motor phase switching frequency. This results in low inverter switching with reduced power circuit complexity when compared to other multilevel inverters.

2. DUAL INVERTER-FED INDUCTION MOTOR WITH OPEN-END WINDING

The schematic of the dual voltage source inverter fed three-phase induction motor with open-end winding is shown in Fig. 1. V_{a0}, V_{b0}, V_{c0} are the pole voltages of the inverter-1. $V_{a'o}, V_{b'o}, V_{c'o}$ are the pole voltages of inverter-2. The space phasor locations from individual inverters are shown in Fig.2. The space phasor combinations from the two inverters are shown in Fig.3. In all 64 space phasor combinations are possible from both the inverters. For example, a combination 6-1' implies that the switching state for inverter-1 is (+ - +) and that for inverter-2 is (+ - -). A '+' means top switch in the inverter is on, a '-' means bottom switch in the inverter is on. The motor phase voltage can be found out from the pole voltages of individual inverters.

Separate DC supply is used for individual inverter to block the flow of third harmonic currents. This is achieved using isolated transformers in providing the DC supply for both the inverters.

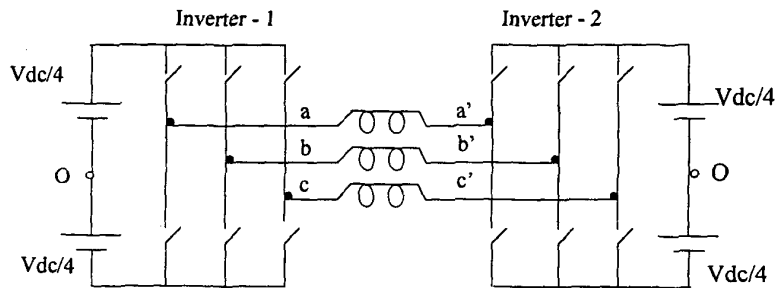


Fig.1 Dual inverter fed 3 phase induction motor with open-end winding.

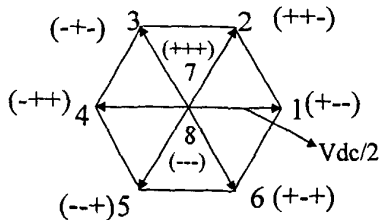


Fig.2(a) Space phasor locations of inverter-1

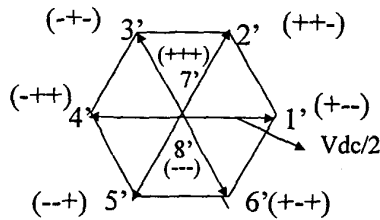


Fig.2(b) Space phasor locations of inverter-2.

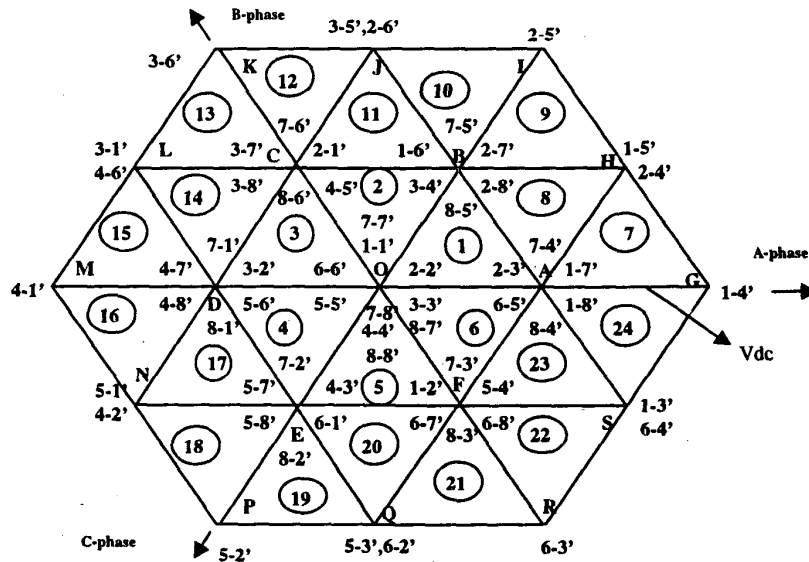


Fig.3 Different Voltage Space Phasor combinations from two inverters.

The 64 voltage space phasor locations form the vertices of 24 equilateral triangles, which are referred to as 24 sectors (Fig.3). Six adjacent sectors together form a hexagon. Six such hexagons can be identified with their centers located at A, B, C, D, E, and F respectively (Fig.4). In addition there is one inner hexagon with its center at O. Based on these sub-hexagons, a space phasor based PWM scheme is proposed in the same way as in the case of the conventional three phase inverter [4].

3. SPACE PHASOR PWM SCHEME FOR THE DUAL INVERTER

As shown in Fig.4, consider the reference voltage vector OT whose tip T lies in sector $S7$. This reference vector OT makes an angle α with A- phase axis. This vector OT can be generated using vectors OA and AT . Vector OT' is exactly similar to vector AT . This vector is generated by switching between the vertices A, G, and H (Fig.3) for a period T_0 , T_1 , and T_2 respectively. Similarly the vector OT' is generated by switching between the vertices O, A, and B for a period T_0 , T_1 , and T_2 respectively. The period T_0 , T_1 , and T_2 remain the same for both the vectors AT and OT' but only the output vectors from the inverters are different. Hence by moving the center of the sub-hexagon A to O (by subtracting the required components along the a, b, c axes respectively), we can calculate T_0 , T_1 , and T_2 for vector OT' in exactly the same way as for a conventional three phase inverter [4].

In the equations (1) to (6), $V_a^*(t)$, $V_b^*(t)$, $V_c^*(t)$ are the sampled phase values of the actual reference vector for the motor phase voltages. To implement the PWM pattern, the triangular sector in which tip of the reference space phasor lies is first identified and sub-hexagon to which it belongs is found out using Fig.5. TABLE-1 gives an example for sector-1 and sector-2 identification. The sector identification is based on hysteresis level comparators along ja , jb , jc axes perpendicular to the a, b, c axes respectively (Fig.5).

After identifying the sub-hexagon its center is moved to the center O of inner hexagon. The new values of V_a , V_b , V_c are calculated using any one of equations (1) to (6) and the phase voltage times T_{as} , T_{bs} , T_{cs} are computed. To generate the actual switching times for each inverter leg, time shifting operation is done as follows. $T_{ga} = T_{as} + T_{offset}$; $T_{gb} = T_{bs} + T_{offset}$; $T_{gc} = T_{cs} + T_{offset}$. Where $T_{zero} = T_s - T_{eff}$, $T_{offset} = T_{zero}/2 - T_{min}$, and $T_s =$ sampling period.

4 PWM PATTERN GENERATION USING 24 TRIANGULAR SECTORS

The entire speed range of operation is divided into 48 sampling intervals (T_s) for the proposed scheme (Fig.6). Further, the speed range is divided into two groups to which the tip of reference space phasor belongs - the outer sub-hexagons (sector S7 to sector S24) or inner hexagon (sector S1 to sector S6). TABLE-3 shows the inverter switching pattern followed for outer sub-hexagons and TABLE-2 for the inner hexagon. For example for sector S7 first the vectors outputted are $18' - 15' - 14' - 17'$ where inverter-1 is clamped to vector 1 while the inverter-2 is in switching mode. This is identified as INV-2 (1-Tg') which indicates that inverter-1 is not switched and inverter-2 is in (1-Tg') mode, where the (1-Tg') mode identified as the switching sequence for inverter-2, is from state-8' for first $T_{zero}/2$ period and state-7' for the last $T_{zero}/2$ period. The Tg' mode is identified as the inverter-2 switching state starting as 7' for first $T_{zero}/2$ period and state-8' as the last $T_{zero}/2$ period. Similar switching sequence for inverter-1 is referred to as INV-1 (1 - Tg) and INV-1 Tg modes (TABLE-3)[4].

In the proposed scheme a switching pattern is evolved in which only one inverter is switched during switching transition and all the 64 space phasor combinations available are made use of for the PWM control covering the entire speed range.

The equations for shifting A to O are

$$\left. \begin{aligned} V_a(t) &= V_a^*(t) - \frac{V_{dc}}{3} \\ V_b(t) &= V_b^*(t) + \frac{V_{dc}}{6} \\ V_c(t) &= V_c^*(t) + \frac{V_{dc}}{6} \end{aligned} \right\} (1)$$

The equations for shifting B to O are

$$\left. \begin{aligned} V_a(t) &= V_a^*(t) - \frac{V_{dc}}{6} \\ V_b(t) &= V_b^*(t) - \frac{V_{dc}}{6} \\ V_c(t) &= V_c^*(t) + \frac{V_{dc}}{3} \end{aligned} \right\} (2)$$

The equations for shifting C to O are

$$\left. \begin{aligned} V_a(t) &= V_a^*(t) + \frac{V_{dc}}{6} \\ V_b(t) &= V_b^*(t) - \frac{V_{dc}}{3} \\ V_c(t) &= V_c^*(t) + \frac{V_{dc}}{6} \end{aligned} \right\} (3)$$

The equations for shifting D to O are

$$\left. \begin{aligned} V_a(t) &= V_a^*(t) + \frac{V_{dc}}{3} \\ V_b(t) &= V_b^*(t) - \frac{V_{dc}}{6} \\ V_c(t) &= V_c^*(t) - \frac{V_{dc}}{6} \end{aligned} \right\} (4)$$

The equations for shifting E to O are

$$\left. \begin{aligned} V_a(t) &= V_a^*(t) + \frac{V_{dc}}{6} \\ V_b(t) &= V_b^*(t) + \frac{V_{dc}}{6} \\ V_c(t) &= V_c^*(t) - \frac{V_{dc}}{3} \end{aligned} \right\} (5)$$

The equations for shifting F to O are

$$\left. \begin{aligned} V_a(t) &= V_a^*(t) - \frac{V_{dc}}{6} \\ V_b(t) &= V_b^*(t) + \frac{V_{dc}}{3} \\ V_c(t) &= V_c^*(t) - \frac{V_{dc}}{6} \end{aligned} \right\} (6)$$

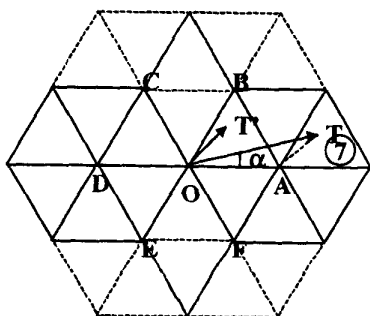


Fig.4 Six sub-hexagons with centres at A,B,C,D,E,F and inner hexagon with centre at 'O'.

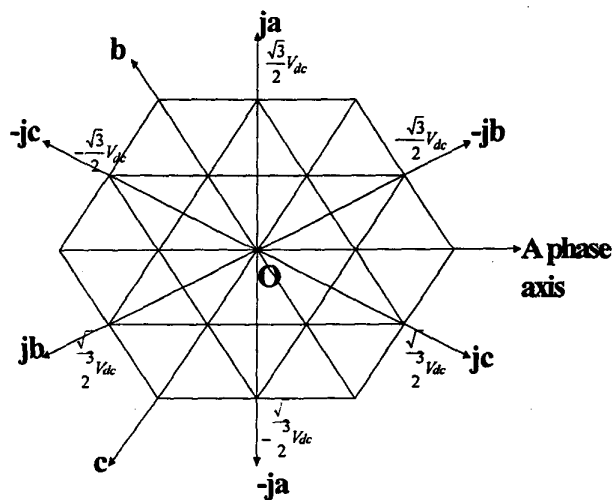


Fig.5 Sector identification using ja, jb, jc axes

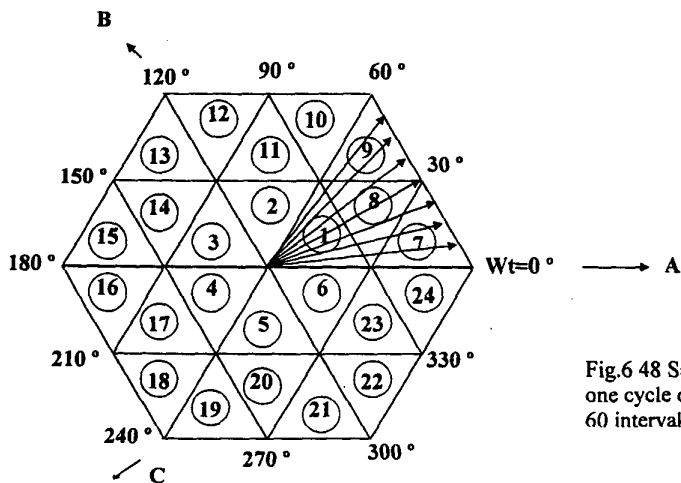


Fig.6 48 Sampling intervals (Ts) for one cycle of operation (8 steps in a 60 interval cycle)

TABLE-1

Sector	Ja	Jb	Jc	Sector	Ja	Jb	Jc
1	$< \frac{\sqrt{3}}{4} V_{dc}$	$\geq -\frac{\sqrt{3}}{4} V_{dc}$	$< \frac{\sqrt{3}}{4} V_{dc}$	2	$< \frac{\sqrt{3}}{4} V_{dc}$	$\geq -\frac{\sqrt{3}}{4} V_{dc}$	$\geq -\frac{\sqrt{3}}{4} V_{dc}$

TABLE-2 SWITCHING SEQUENCE WHEN TIP OF THE REFERENCE VECTOR LIES IN THE INNER HEXAGON

SECTOR NO.	INV-1 NOT SWITCHED				INV-2 NOT SWITCHED				
	T0/2	T1	T2	T0/2	T0/2	T1	T2	T0/2	
S1	88°	85°	84°	87°	87°	17°	27°	77°	Positive sequence Wt = 30°
	$(1 - Tg')$ →				$(1 - Tg)$ →				
S1	77°	74°	75°	78°	78°	28°	18°	88°	Negative sequence Wt = 90°
S2	77°	76°	75°	78°	78°	28°	38°	88°	
	Tg' →				Tg →				
S2	88°	85°	86°	87°	87°	37°	27°	77°	Positive sequence Wt = 150°
S3	88°	81°	86°	87°	87°	37°	47°	77°	
	$(1 - Tg')$ →				$(1 - Tg)$ →				
S3	77°	76°	71°	78°	78°	48°	38°	88°	Negative sequence Wt = 210°
S4	77°	72°	71°	78°	78°	48°	58°	88°	
	Tg' →				Tg →				
S4	88°	81°	82°	87°	87°	57°	47°	77°	Positive sequence Wt = 270°
S5	88°	83°	82°	87°	87°	57°	67°	77°	
	$(1 - Tg')$ →				$(1 - Tg)$ →				
S5	77°	72°	73°	78°	78°	68°	58°	88°	Negative sequence Wt = 330°
S6	77°	74°	73°	78°	78°	68°	18°	88°	
	Tg' →				Tg →				
S6	88°	83°	84°	87°	87°	17°	67°	77°	Positive sequence

To facilitate the above, the switching sequence is divided into positive sequence and negative sequence as per TABLE-2 and TABLE-3. The change over from positive sequence to negative sequence occurs at $wt = 30^\circ, 150^\circ, 270^\circ$. Similarly the change over from negative sequence to positive sequence starts at $wt = 90^\circ, 210^\circ, 330^\circ$. The change from positive sequence to negative sequence or vice versa is achieved by only one inverter leg switching.

5. EXPERIMENTAL RESULTS

The proposed scheme is simulated using MATLAB and SIMULINK software for a 5 H.P., 3 Phase induction motor drive in open loop with V/f control for different reference voltages covering the entire speed range. Fig.7a shows the pole voltages of the individual inverters (Vao and Va'o) for reference space phasor voltage $V_{sr} = 1.0$ Vdc (over-modulation). Fig.7b shows the motor phase voltage Vaa' (upper trace) and its third harmonic content (lower trace) for $V_{sr} = 1.0$ Vdc. Fig.8a shows the pole voltages for $V_{sr} = 0.7$ Vdc and Fig.8b shows the motor phase voltage Vaa' (upper trace) and its third harmonic content (lower trace) for $V_{sr} = 0.7$ Vdc. The proposed scheme is also simulated for a reference space phasor voltage $V_{sr} = 0.4$ Vdc and the results are shown in Figs.9a and 9b respectively. The proposed scheme is tested for a 5 H.P., 3 Phase induction motor drive with open-end winding using transformer isolation (for the front end rectifier) for third harmonic filtering. Fig.10 shows the motor phase

voltage without third harmonic (upper trace) and current waveform (lower trace) for reference space phasor voltage $V_{sr} = 1.0$ Vdc. Fig.11 shows the motor phase voltage without third harmonic and current waveform for $V_{sr} = 0.7$ Vdc and Fig.12 shows the motor phase voltage without third harmonic and current waveform for $V_{sr} = 0.4$ Vdc.

The salient features of the proposed scheme are

- The voltage space phasor locations are similar to 3-level inverter.
- In all 64 space phasor locations are possible for the present scheme as compared to 27 for a 3-level inverter.
- Two 2-level inverters with half the DC link voltage are needed for the present scheme.
- Total number of switching power devices is less for the proposed scheme when compared to 3-level inverter.
- A PWM scheme is proposed making use of all the space phasor combinations covering the entire speed range.
- Only one inverter leg is switched during a sub-cycle of operation of a sampling interval.

Each inverter switching frequency is equal to half of that of the motor phase switching frequency.(if 'n' is the total number of switching in a cycle of operation then each

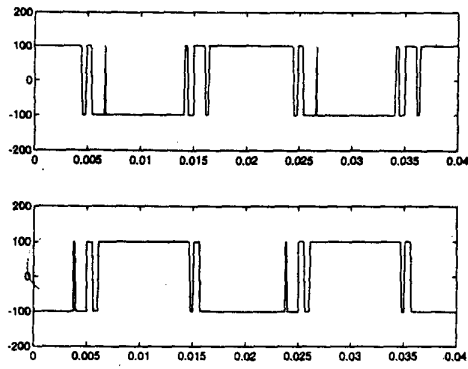


Fig.7a. Pole voltages V_{a0} and $V_{a'0}$
During overmodulation ($V_{sr} = 1.0V_{dc}$)

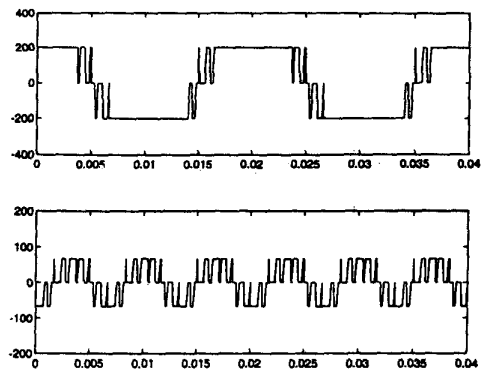


Fig.7b. Motor phase voltage $V_{aa'}$ and
 3^{rd} harmonic content- overmodulation

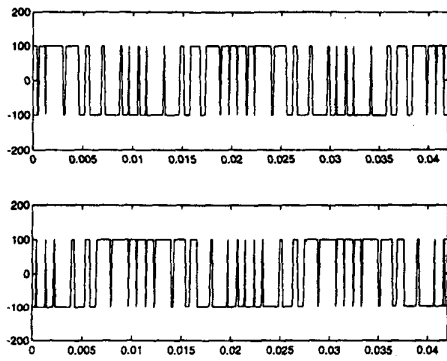


Fig.8a. Pole voltages V_{a0} and $V_{a'0}$
For $V_{sr} = 0.7V_{dc}$

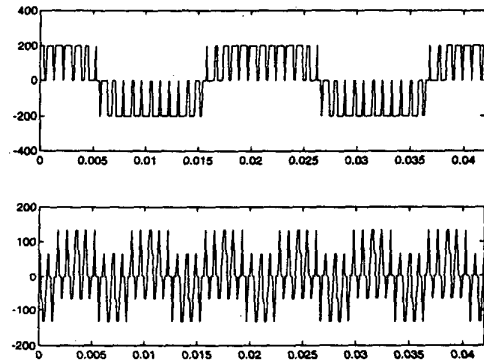


Fig.8b. Motor phase voltage $V_{aa'}$ and
 3^{rd} harmonic content- $V_{sr} = 0.7V_{dc}$

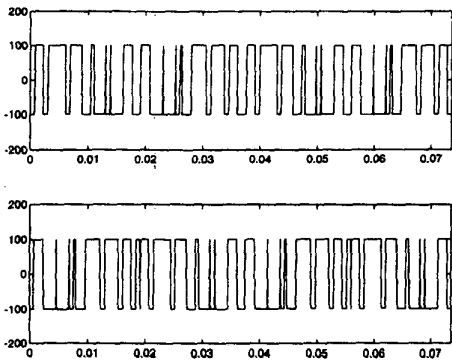


Fig.9a. Pole voltages V_{a0} and $V_{a'0}$
For $V_{sr} = 0.4V_{dc}$

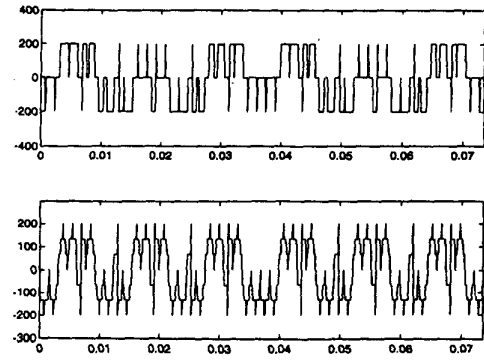


Fig.9b. Motor phase voltage $V_{aa'}$ and
 3^{rd} harmonic content- $V_{sr} = 0.4V_{dc}$

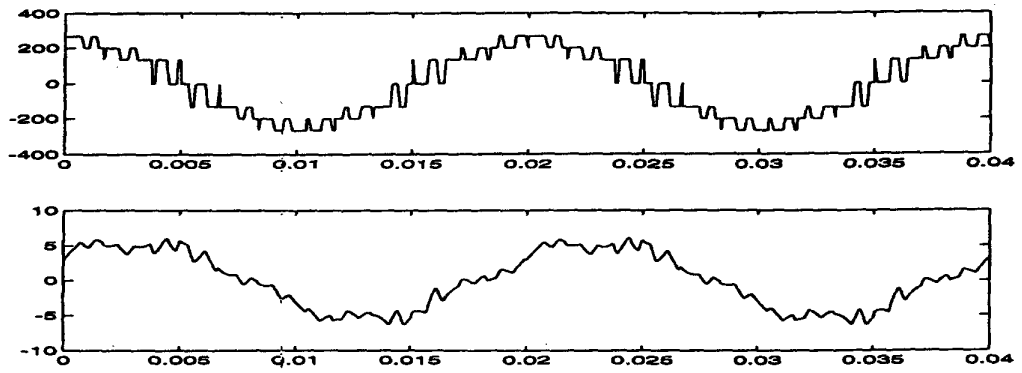


Fig.10. Motor phase voltage(with out third harmonic) and current for $V_{sr}=1.0V_{dc}$

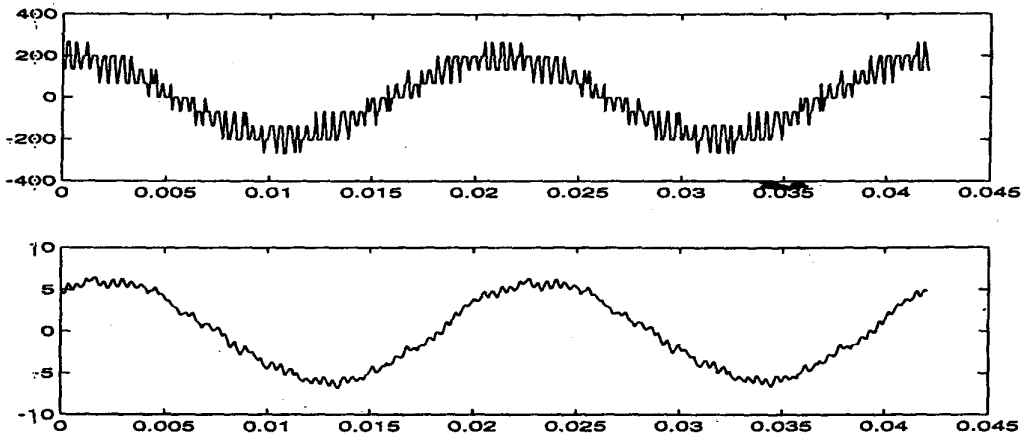


Fig.11. Motor phase voltage(with out third harmonic) and current for $V_{sr}=0.7V_{dc}$

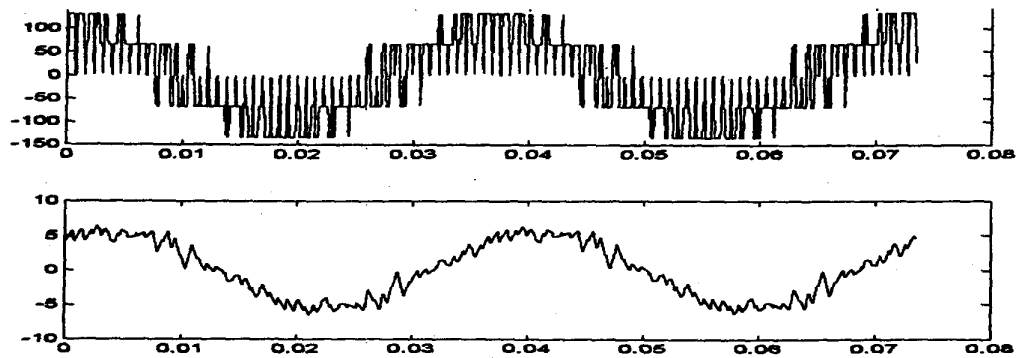


Fig.12. Motor phase voltage(with out third harmonic) and current for $V_{sr}=0.4V_{dc}$

TABLE-3: SWITCHING SEQUENCE WHEN TIP OF THE REFERENCE VECTOR LIES IN ANY OF THE OUTER SUB-HEXAGONS

SEC TOR NO.	INV-1 NOT SWITCHED				INV-2 NOT SWITCHED				
	T0/2	T1	T2	T0/2	T0/2	T1	T2	T0/2	
S23	18'	13'	12'	17'	84'	54'	64'	74'	sub-hexagon origin 'A' is shifted to 'O' positive sequence wt = 30 °
S24	18'	13'	14'	17'	84'	14'	64'	74'	
S07	18'	15'	14'	17'	84'	14'	24'	74'	
S08	18'	15'	16'	17'	84'	34'	24'	74'	
	$(1 - Tg')$ →				$(1 - Tg)$ →				
S08	27'	24'	23'	28'	75'	65'	15'	85'	sub-hexagon origin 'B' is shifted to 'O' negative sequence wt = 90 °
S09	27'	24'	25'	28'	75'	25'	15'	85'	
S10	27'	26'	25'	28'	75'	25'	35'	85'	
S11	27'	26'	21'	28'	75'	45'	35'	85'	
	Tg' →				Tg →				
S11	38'	35'	34'	37'	86'	16'	26'	76'	sub-hexagon origin 'C' is shifted to 'O' positive sequence wt = 150 °
S12	38'	35'	36'	37'	86'	36'	26'	76'	
S13	38'	31'	36'	37'	86'	36'	46'	76'	
S14	38'	31'	32'	37'	86'	56'	46'	76'	
	$(1 - Tg')$ →				$(1 - Tg)$ →				
S14	47'	46'	45'	48'	71'	21'	31'	81'	sub-hexagon origin 'D' is shifted to 'O' negative sequence wt = 210 °
S15	47'	46'	41'	48'	71'	41'	31'	81'	
S16	47'	42'	41'	48'	71'	41'	51'	81'	
S17	47'	42'	43'	48'	71'	61'	51'	81'	
	Tg' →				Tg →				
S17	58'	51'	56'	57'	82'	32'	42'	72'	sub-hexagon origin 'E' is shifted to 'O' positive sequence wt = 270 °
S18	58'	51'	52'	57'	82'	52'	42'	72'	
S19	58'	53'	52'	57'	82'	52'	62'	72'	
S20	58'	53'	54'	57'	82'	12'	62'	72'	
	$(1 - Tg')$ →				$(1 - Tg)$ →				
S20	67'	62'	61'	68'	73'	43'	53'	83'	sub-hexagon origin 'F' is shifted to 'O' negative sequence wt = 330 °
S21	67'	62'	63'	68'	73'	63'	53'	83'	
S22	67'	64'	63'	68'	73'	63'	13'	83'	
S23	67'	64'	65'	68'	73'	23'	13'	83'	
	Tg' →				Tg →				

- inverter will be switched for 'n/2' times only during one cycle of operation). [5]

6. REFERENCES

[1] A.Nabae, I.Takahashi, and H.Agaki,"A new neutral-point-clamped PWM inverter", IEEE Trans.Ind.Applicat.,vol.IA-17,pp518-523,sept./oct. 1981

[2] P.M.Bhagwat and V.R.Stefanovic,"Generalized Structure of a multi level PWM inverter", IEEE Trans.Ind.Applicat.vol.IA-19,pp1057-1069,Nov./Dec.1983.

[3] H.Stemmler, P.Guggenbach,"Configurations of high power voltage source inverter drives", EPE.conf-1993,pp7-12.

[4] Joohn-Sheok Kim,Seung-Ki Sul," A Novel Voltage Modulation Technique of the Space Vector PWM",IPEC-1995,pp742-747.

Bakari Mwinyiwiwa, Zbigniew Wolanski,"Multimodular Multilevel Converters with Input/Output Linearity", IEEE Trans.Ind.Applicat., vol.33,No.5, sept./oct. 1997,pp 1214-1219.

[6] A.Rufer, M.Veenstra, K.Gopakumar,"Asymmetric multilevel converter for high resolution voltage phasor generation", EPE'99-Lausanne,pp.P1-P10.

APPENDIX - A

Motor parameters:-5HP 3-phase IM

$R_s = 2.08$ ohms; $R_r = 4.19$ ohms;
 $M = 0.272$ H; $\sigma = 0.0294$;
 $L_s = 0.28$ H; $L_r = 0.28$ H;
 $J = 0.11$ Kg-m²; $p = 4$